Inorg. Chem. **2002**, *41*, 5770–5777

ZINDO Calculations of the Ground State and Electronic Transitions in the Tetracyanonickelate Ion, $Ni(CN)_4^{2-}$

Yves A. Mantz[†] and Ronald L. Musselman*

Department of Chemistry, Franklin and Marshall College, Lancaster, Pennsylvania 17604

Received June 18, 2002

ZINDO semiempirical calculations on the $Ni(CN)_4^{2-}$ ion were performed, and ground-state energies for all 41 valence-orbital-based MOs and orbital transition components of the two lowest energy fully allowed electronic transitions are reported. Gaussian 94 was used to calculate ground-state energies as a comparison. The ground-state energies using ZINDO compare much more favorably with those found through ab initio techniques than with those from a reported INDO calculation. The found electronic transitions agree substantially with earlier assignments with the exception that several orbital transitions are required to adequately model the lowest energy allowed *x*,*y*-polarized experimental transition. Calculation parameters were optimized to give excellent agreement with experiment and may serve well for more complex arrangements of this ion.

Introduction

The tetracyanonickelate ion has generated a great deal of interest over several decades on its own[1−11] as well as from being a member of one-dimensional solid-state systems which are of interest with regard to one-dimensional conductivity.[12−14] Recent interest in this complex includes cocrystallization with tris(ethylenediamine)nickel(II)[15] and Fe(methylpyridine),[16] one-dimensional ladder structures,[17] simple modeling for more complex systems such as substituted phthalocyanines which are used in photovoltaic devices,[18] and applications as tumor imaging agents.[19] The planar tetracyanometalates are most notable for the dramatic red-shifting and intensity increase of the prominent low-energy charge-transfer transitions, $A_{1g} \rightarrow A_{2u}$ (a_{1g} (d_{z^2}) → a_{2u} (p_z, π^*)) and $A_{1g} \rightarrow E_u$ (e_g (d_{xz}, d_{yz}) → a_{2u} (p_z, π^*)), when the planes are subjected to external pressure[20−22] or when cocrystallized with various cations to give closer planar stacking.[6,23−25] They also have interesting electrical properties.[7,26,27] Our eventual goal is to model the spectral perturbations in aggregates of these complexes.

Numerous studies of the electronic structure of the single $Ni(CN)_4^{2-}$ ion have been reported, including a molecular orbital study,[2] several ab initio calculations,[5,28,29] and an early

* To whom correspondence should be addressed. E-mail: Ronald.Musselman@fandm.edu.

[†] Current address: IBM T. J. Watson Research Center, P.O. Box 218, Yorktown Heights, NY 10598-0218.

(1) Perumareddi, J. R.; Liehr, A. D.; Adamson, A. W. *J. Am. Chem. Soc.* **1963**, *85*, 249.
(2) Gray, H. B.; Ballhausen, C. J. *J. Am. Chem. Soc.* **1963**, *85*, 260.
(3) Haines, R. A.; Smith, A. A. *Can. J. Chem.* **1968**, *46*, 1444.
(4) Holt, E. M.; Watson, K. J. *Acta Chem. Scand.* **1969**, *23*, 14.
(5) Demuynck, J.; Veillard, A. *Theor. Chim. Acta*, **1973**, *28*, 241.
(6) Cowman, C. D.; Ballhausen, C. J.; Gray, H. B. *J. Am. Chem. Soc.* **1973**, *95*, 7873.
(7) Musselman, R. L.; Cornelius, J. B.; Trapp, R. M. *Inorg. Chem.* **1981**, *20*, 1931.
(8) Gainsford, G. J.; Curtis, N. F. *Aust. J. Chem.* **1984**, *37*, 1799.
(9) Kumar, K.; Bajaj, H. C.; Nigam, P. C. *J. Phys. Chem.* **1980**, *84*, 2351.
(10) Dowling, J. P. *Acta Chem. Scand.* **1992**, *23*, 14.
(11) Banciu, A. C. *Rev. Roum. Chim.* **1999**, *44*, 889.
(12) Johnson, P. L.; Musselman, R. L.; Williams, J. M. *Acta Crystallogr., Sect. B* **1977**, *33*, 3155.
(13) Stucky, G. D.; Schultz, A. J.; Williams, J. M. *Annu. Rev. Mater. Sci.* **1977**, *7*, 301.
(14) Keller, H. J. *Comments Inorg. Chem.* **1981**, *1*, 71.
(15) Cernak, J.; Potocnak, I.; Dunaj-Jurco, M. *Z. Kristallogr.* **1994**, *209*, 757.
(16) Kitazawa, T.; Eguchi, M.; Takeda, M. *Mol. Cryst. Liq. Cryst.* **2000**, *341*, 1331.
(17) Knoeppel, D. W.; Shore, S. G. *Inorg. Chem.* **1996**, *35*, 5328.
(18) McHale, G.; Newton, M. I.; Hooper, P. D.; Willis, M. R. *Opt. Mater.* **1996**, 89.
(19) Mang, T. S.; McGinnis, C.; Liebow, C.; Nseyo, U. O.; Crean, D. H.; Dougherty, T. J. *Cancer*, **1993**, *71*, 269.
(20) Yersin, H.; Gliemann, G. *Z. Naturforsch. B: Chem. Sci.* **1975**, *30*, 183.
(21) Yersin, H.; Gliemann, G. *Ann. N.Y. Acad. Sci.* **1978**, *313*, 539.
(22) Lechner, A.; Gliemann, G. *J. Am. Chem. Soc.* **1989**, *111*, 7469.
(23) Moreau-Colin, M. L. *Bull. Soc. Chim. Belg.* **1965**, *51*, 916.
(24) Moreau-Colin, M. L. *Bull. Soc. Chim. Belg.* **1965**, *34*, 772.
(25) Moreau-Colin, M. L. *Struct. Bonding (Berlin)* **1972**, *10*, 167.
(26) Jasin, J.; Cornelius, J. B.; Watkins, S. F.; Fronczek, F.; Musselman, R. L. Unpublished work.
(27) Musselman, R. L.; Williams, J. W. *J. Chem. Soc., Chem. Commun.* **1977**, 186.
(28) Hillier, I. H.; Saunders, V. R. *Mol. Phys.* **1972**, *23*, 449.
(29) Sano, M.; Kashiwagi, H.; Yamatera, H. *Bull. Chem. Soc. Jpn.* **1982**, *55*, 750.

10.1021/ic025798x CCC: $22.00
Published on Web 10/10/2002

semiempirical calculation.[30] Because aggregations of such complexes are difficult to study with ab initio techniques, it seems reasonable to attempt the modeling with an approximation technique such as ZINDO, the improved semiempirical INDO calculation developed by Zerner and others.[31] The more complex porphyrins[32] and phthalocyanines[33,34] have been modeled successfully by this method. No treatment of $Ni(CN)_4^{2-}$ using the ZINDO technique has appeared to our knowledge, and it thus seems reasonable to study this ion carefully using ZINDO, with the objective of determining the parameters which give the best fit to experimental spectra for the two transitions of interest before attempting to study aggregated systems.

In 1963, Perumareddi et al.[1] studied several metal cyanides including $Ni(CN)_4^{2-}$ but did not assign charge transitions specifically. Gray and Ballhausen[2] proposed a ligand orbital scheme for square-planar complexes containing unsaturated ligands, and in 1968, Mason and Gray interpreted a $Ni(CN)_4^{2-}$ spectrum in confirmation of this scheme.[35] The lowest energy allowed transition was assigned as an $A_{1g} \rightarrow A_{2u}$ (a_{1g} (d_{z^2}) $\rightarrow$ a_{2u} (p_z, π^*)) transition (allowed with the electric vector aligned perpendicular to the molecular plane ("*z*-polarized")), and the next lowest energy transition as $A_{1g} \rightarrow E_u$ (e_g (d_{xz}, d_{yz}) $\rightarrow$ a_{2u} (p_z, π^*)) (allowed parallel to the molecular plane ("*x*,*y*-polarized")). Through MCD (magnetic circular dichroism) spectra of $K_2Ni(CN)_4$ in solution, Stephens et al.[36] confirmed the assignments of the $A_{1g} \rightarrow A_{2u}$ and $A_{1g} \rightarrow E_u$ transitions. Polarized absorption spectra of various forms of $Ni(CN)_4^{2-}$ were reported by Ballhausen et al.[6,37] Their 1965 paper[37] reported on several salts of $Ni(CN)_4^{2-}$, all of which were perturbed by the crystal structures. In their 1973 paper,[6] they reported a polarized absorption liquid helium study of tetrabutylammonium tetracyanonickelate which showed remarkable resolution of transitions and basically confirmed the major two transitions' polarization assignments of earlier work. In addition, evidence of spin−orbit coupled states was apparently made prominent at this low temperature where it had been difficult to see at even slightly higher temperatures. The crystal structure of the thin films studied, however, was not identified either in the paper or in a more detailed report.[38] A few years later, our laboratory experimentally found polarizations of these transitions via specular reflectance spectroscopy on the CsK salt of $Ni(CN)_4^{2-}$,[39] whose structure placed the Ni−Ni distance at 4.20 Å, and the spectra showed essentially no solid-state perturbation. We found that the lowest energy allowed electronic transition was indeed *z*-polarized and the next lowest was *x*,*y*-polarized. Some years later, we found experimentally some anomalous behavior of the lowest energy in-plane transitions in solid-state mixed $Ba[Ni(CN)_4]_x[Pt(CN)_4]_{1-x}\cdot 4H_2O$.[40] We suggested that the lowest energy Ni transition appeared to be due to a $b_{2g}(d_{xy}) \rightarrow e_u(p_x, p_y, \pi^*)$ orbital transition. Mason[41] pointed out that MCD data still strongly pointed to the original assignment in the single molecule but that there seemed to be no obvious explanation for our reported solid-state results. Very recently, an additional interpretation of $Ni(CN)_4^{2-}$ spectra appeared,[11] but it focuses on the d−d and spin-forbidden transitions that are not within the scope of this paper. This paper serves as a foundation for theoretical study of the solid-state spectral perturbations in $Ni(CN)_4^{2-}$ systems and reports our use of ZINDO to calculate the ground-state energies and electronic transitions for $Ni(CN)_4^{2-}$ and Gaussian 94[42] to calculate ground-state energies for $Ni(CN)_4^{2-}$ as a comparison.

Method

Ab Initio Calculations. Because we want to compare the orbital calculations from ZINDO with those of more complex ab initio calculations, we performed Gaussian 94 calculations[42] to update earlier ab initio calculations.[5,28,29] We performed an all-electron geometry optimization of $Ni(CN)_4^{2-}$ constrained to D_{4h} symmetry at the MP2 level of theory with a 6-311+G basis set (including diffuse functions on all atoms, for a total of 187 basis functions and 318 primitive Gaussians). The two degrees of freedom in the calculation were given initial values of d(Ni−C) = 1.86 Å and d(C−N) = 1.15 Å identical to the values chosen by Demuynck et al.[5] and Sano[29] for their static calculations.

Semiempirical Calculations. Both ground-state energies and allowed electronic transitions were calculated using the Zerner-modified semiempirical INDO (Intermediate Neglect of Differential Overlap) method known as ZINDO.[31] The version of ZINDO we use here is contained in the CAChe suite of programs from Fujitsu.[43] The program is also available from Accelrys[44] and Hypercube, Inc.[45] It has been very successful in interpreting the electronic structures of a wide variety of organometallic molecules, including ferrocene[46] and porphryins.[32] The CAChe implementation of ZINDO has been used recently by Gouterman et al. on a substituted porphyrin[47] and by Stillman and Mack on phthalocyanines.[48] Because the ZINDO technique is semiempirical, the calculation parameters typically need

(30) Zeigler, T. *Acta Chem. Scand.* **1974**, *28*, 29.
(31) Ridley, J.; Zerner, M. *Theor. Chim. Acta.* **1973**, *32*, 111.
(32) Edwards, W. D.; Weiner, B.; Zerner, M. C. *J. Am. Chem. Soc.* **1986**, *108*, 2196.
(33) Soares, L.d.A.; Trsic, M.; Berno, B.; Aroca, R. *Spectrochim. Acta, Part A* **1996**, *52*, 1245.
(34) Mack, J.; Stillman, M. J. *J. Porphyrins Phthalocyanines* **2001**, *5*, 67.
(35) Mason, W. R.; Gray, H. B. *J. Am. Chem. Soc.* **1968**, *90*, 5721.
(36) Stephens, J. P.; McCaffery, A. J.; Schatz, P. N. *Inorg. Chem.* **1968**, *7*, 1923.
(37) Ballhausen, C. J.; Bjerrum, N.; Dingle, R. *Inorg. Chem.* **1965**, *4*, 514.
(38) Cowman, C. Ph.D. Dissertation, California Institute of Technology, 1974.
(39) Musselman, R. L.; Stecher, L. C.; Watkins, S. F. *Inorg. Chem.* **1980**, *19*, 3400.
(40) Arndt, G. A.; Danielson, E. D.; Fanta, A. D.; Musselman, R. L. *Inorg. Chem.* **1988**, *27*, 1400.
(41) Mason, W. R. *Inorg. Chem.* **1989**, *28*, 2487.
(42) Frisch, M. J.; Trucks, G. W.; Schlegel, H. B.; Gill, P. M. W.; Johnson, B. G.; Robb, M. A.; Cheeseman, J. R.; Keith, T.; Petersson, G. A.; Montgomery, J. A.; Raghavachari, K.; Al-Laham, M. A.; Zakrzewski, V. G.; Ortiz, J. V.; Foresman, J. B.; Cioslowski, J.; Stefanov, B. B.; Nanayakkara, A.; Challacombe, M.; Peng, C. Y.; Ayala, P. Y.; Chen, W.; Wong, M. W.; Andres, J. L.; Replogle, E. S.; Gomperts, R.; Martin, R. L.; Fox, D. J.; Binkley, J. S.; Defrees, D. J.; Baker, J.; Stewart, J. P.; Head-Gordon, M.; Gonzalez, C.; Pople, J. A. *Gaussian 94*, revision E.3; Gaussian, Inc.: Pittsburgh, PA, 1995.
(43) Zerner, M. C. *ZINDO (in CAChe)*; Fujitsu Limited: Beaverton, OR, 2000.
(44) Zerner, M. C. *ZINDO (in Cerius2)*; Accelrys: San Diego, CA, 1998.
(45) Zerner, M. C. *ZINDO (in HyperChem)*, Hypercube, Inc.: Gainesville, FL, 1996.
(46) Zerner, M. C.; Loew, G. H.; Kirchner, R. F.; Mueller-Westerhoff, U. T. *J. Am. Chem. Soc.* **1980**, *102*, 589.
(47) Vitasovic, M.; Gouterman, M.; Linschitz, H. *J. Porphyrins Phthalocyanines* **2001**, *5*, 191.
(48) Mack, J.; Stillman, M. J. *Inorg. Chem.* **1997**, *36*, 413.

to be optimized in order for the calculated electronic spectrum to match the experimental spectrum as closely as possible. This paper will include the method of parameter selection for $Ni(CN)_4^{2-}$.

The CACheimplementation of ZINDO includes default values for numerous parameters. The parameters most commonly adjusted in transition metal complexes are the resonance integrals for the central metal, β_s, β_p, and β_d.[49] β_s and β_p are set equal ("β_{sp}") and represent the amount of interaction between s and p orbitals on the metal and those on adjacent ligand atoms. The β_d values represent interaction of the metal d orbitals with ligands. Values of β_{sp} for Ni have ranged from -1[49] to -32,[50,51] and values of β_d for Ni have ranged from -29[43] to -45.[49] Values which are more negative represent a greater interaction between the corresponding metal orbital(s) and the ligand orbitals. The values of the β_{sp} and β_d parameters suitable for the single molecule were determined by closest agreement of the resulting calculated electronic absorption spectrum with experiment. The same method was used for determining the most appropriate level of configuration interaction (CI).

The CI level in this case affected only the state transitions and not the individual orbital energies or wave functions. The ZINDO CI in CACheis a monoexcited CI (i.e., includes only single excitations or singly excited determinants). According to Brillouin's theorem, single excitations do not mix directly with the Hartree−Fock approximation to the ground state, and their contribution to the correlation energy is zero. Because we are determining appropriate parameters on the basis of best spectral matching and we are presenting orbital energy and wave function results before the transition energy results, we simply report at this point that the most suitable CI level was found to be 10. The details leading to this choice will be presented in the state transition section of this paper. We list the ZINDO parameters used in the Supporting Information (SI), Table S-1.

The molecular structure used was an issue, but, as shown later, was not a major issue. Crystal structures containing tetracyanonickelate ions have slight variations from D_{4h} symmetry.[4,8,10,15,16,52−55] The advantage of using a "real" structure as opposed to an idealized (exactly D_{4h}) structure would be a more realistic basis for the calculation. A disadvantage is that symmetry relationships such as degenerate orbitals would not be evident. In our experience, we found an additional disadvantage to the use of a real structure: the optimum degree of configuration interaction (CI) happens to be available only with the ideal structure. We will describe this in greater detail when discussing the procedure for configuration interaction optimization. We chose as an ideal structure a square plane with bond distances equal to the average values in $Ba[Ni(CN)_4]\cdot 4H_2O$:[53] d(Ni−C) = 1.860 Å, d(C−N) = 1.154 Å, Table S-2.

In using experimental spectra as a measure of the accuracy of the calculations, an appropriate spectrum must be used. The solution spectrum of $Ni(CN)_4^{2-}$ would be a logical choice, but it has additional transitions in the region of interest besides those of primary interest, such as vibronic components[39] and a peak

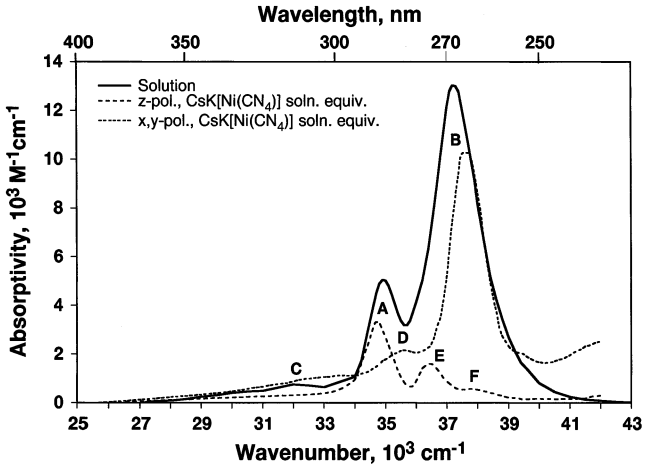

Figure 1. Polarized absorbance spectra of $CsK[Ni(CN)_4]$[39] compared with the solution spectrum of the $Ni(CN)_4^{2-}$ ion.

apparently due to spin−orbit coupling.[56] Additionally, peak broadening due to collision with solvent molecules is an added complication. A better candidate is our polarized absorption spectrum of an unperturbed $Ni(CN)_4^{2-}$ salt,[39] which allows the separation of *x*,*y*-polarized peaks from *z*-polarized ones. (Another advantage is that solvent effects are also eliminated, but minor perturbations from adjacent planes and ions may have replaced the solvent effects because the peaks have very similar shapes.) The *x*,*y*-polarized and *z*-polarized absorptions of $CsK[Ni(CN)_4]$ are reproduced along with the solution spectrum in Figure 1. It is clear that the prominent peak labeled A is allowed *z* and appears to be the lowest energy $A_{1g} \rightarrow A_{2u}$ transition, and peak B is allowed *x*,*y* and appears to be an $A_{1g} \rightarrow E_u$ transition; these are the two transitions of interest here. The additional peaks that appear under the envelope of the solution spectrum are C, which may be the symmetry-forbidden charge-transfer transition $2b_{1g} \rightarrow 4a_{2u}$,[36] D, which may be a result of spin−orbit coupling derived from the $A_{1g} \rightarrow A_{2u}$ transition in peak B,[56] and E and F, vibrational components of peak A.[39] Because ZINDO calculations model only orbitally allowed transitions, provide transition intensities for only spin-allowed transitions, and do not consider spin−orbit coupling, we will compare the calculated transitions with the pure orbitally allowed singlet−singlet transitions represented by peaks A and B in Figure 1.

Results and Discussion

Ab Initio Ground-State Calculations. The results of the calculation which, to our knowledge, represent the first published geometry optimization of $Ni(CN)_4^{2-}$ are the following: d(Ni−C) = 1.840 Å, d(C−N) = 1.208 Å; E(RHF) = −1875.89021732 au; E(MP2) = −1877.1426502 au. Our optimized bond lengths agree to within a few hundredths of one angstrom with the experimental values cited in the early ab initio papers[5,29] and further validate our choice of ab initio method and basis set. The energies of selected orbitals around the Fermi level are shown in the left half of Figure 2. The energies of the filled orbitals are similar to previous reports of ab initio calculations[5,28,29] which were LCAO-MO-SCF calculations using Gaussian basis sets, but the virtual orbitals are somewhat lower than the one case where virtual orbitals had been reported.[5] A complete list of the energies of 187 orbitals is given in the SI, Table S-3.

(49) Anderson, W. P.; Edwards, W. D.; Zerner, M. C. *Inorg. Chem.* **1986**, *25*, 2728.
(50) Allen, G. C.; Clack, D. W. *J. Chem. Soc.* **1970**, 2668.
(51) Clack, D. W.; Farrimond, M. S. *J. Chem. Soc.* **1971**, 299.
(52) Basson, S. S.; Bok, L. D.; Leipoldt, J. G. *Acta Crystallogr., Sect. B* **1969**, *25*, 579.
(53) Larsen, F. K.; Hazell, R. G.; Rasmussen, S. E. *Acta Chem. Scand.* **1969**, *23*, 61.
(54) Leipoldt, J. G.; Basson, S. S.; Bok, L. D. *Acta Crystallogr., Sect. B* **1970**, *26*, 361.
(55) Bok, L. D. C.; Basson, S. S.; Leipoldt, J. G.; Wessels, G. F. S. *Acta Crystallogr., Sect. B* **1971**, *27*, 1233.
(56) Piepho, S. B.; Schatz, P. N.; McCaffery, A. J. *J. Am. Chem. Soc.* **1969**, *91*, 5994.

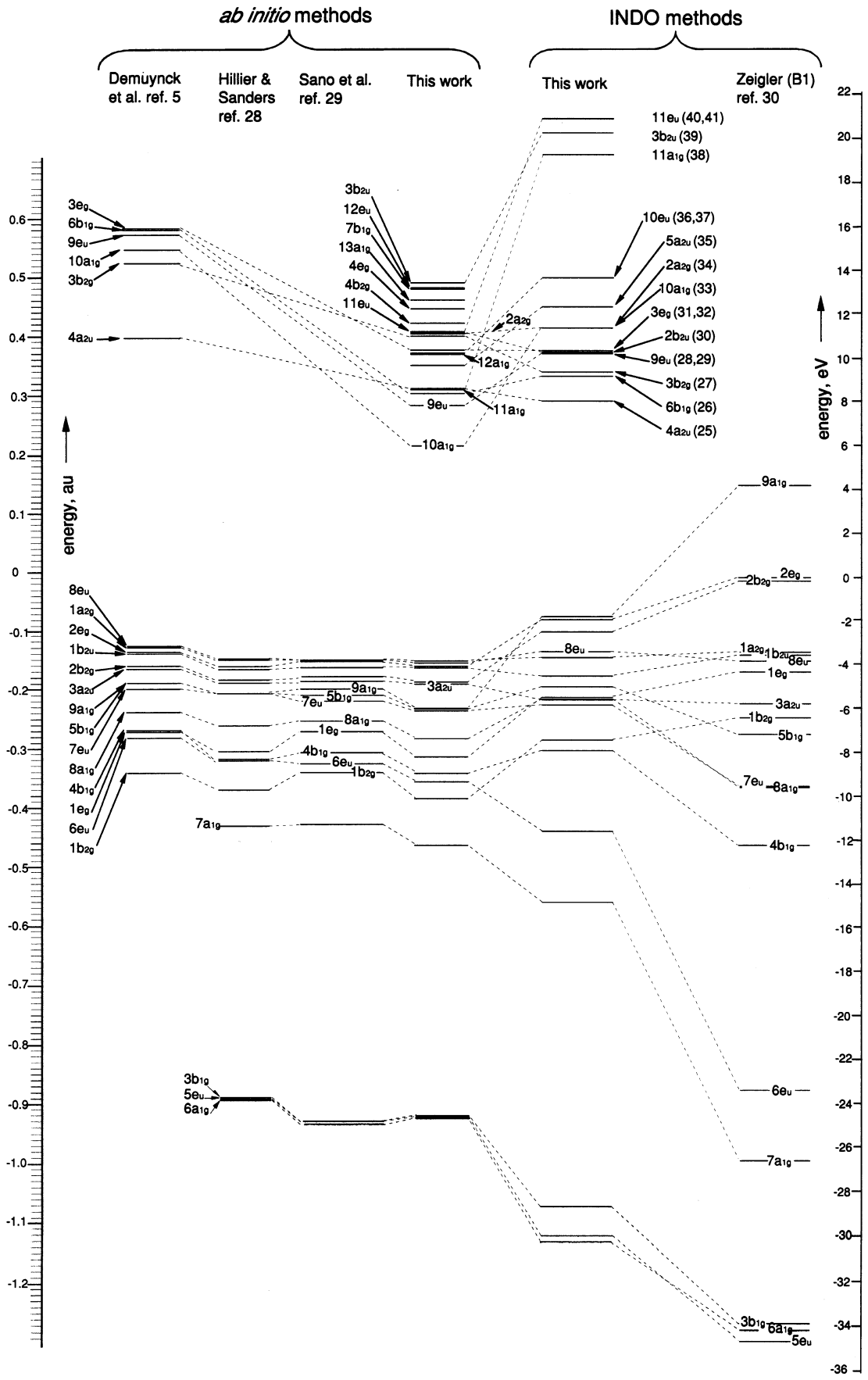

Figure 2. Ab initio and parametrized calculation results. From left: Demuynck et al.,[5] Hillier and Sanders,[28] Sano et al.,[29] and this work using Gaussian 94[42] (ab initio); this work using ZINDO[43] and Zeigler using INDO[30] (INDO methods).

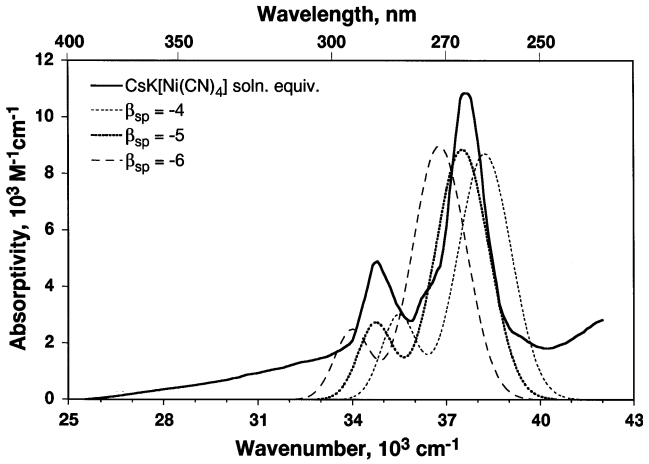

Figure 3. Comparison of the effect of varying β_{sp} values on the calculated absorption spectrum of the $Ni(CN)_4^{2-}$ ion, compared with a solution-equivalent summation of the polarized spectra of $CsK[Ni(CN)_4]$.[39]

ZINDO Ground-State Calculations. Using a CI level of 10, we modified the values of the β_{sp} and β_d parameters. The results were that variations in β_d had no significant effect on the energies or wave functions but the β_{sp} values had a dramatic effect. We thus used the default value of -41 for the nickel β_d. The default value for nickel's β_{sp} was -1; we show the spectral results for values from -4 though -6 in Figure 3, in which it is clear that the optimum value is -5.

The ground-state calculation with this optimized β_{sp} on the ideal geometry of $Ni(CN)_4^{2-}$ used only valence orbitals; a summary of the energies of the resulting 41 wave functions with symmetries is given in the SI, Table S-4 (calculated with CI = 10, vide infra), and the complete molecular orbital wave functions in terms of Ni, C, and N atomic orbitals are listed in Table S-5. In Figure 4, for selected MOs, we have indicated the major contribution from the Ni orbitals and graphic depictions of the orbitals. The complete set of MOs is illustrated in the SI, Figure S-1.

The energies calculated for the 41 MOs using valence orbitals are plotted in the right portion of Figure 2 along with those found in several previous calculations including our ab initio results. While the ZINDO results are similar to the ab initio results, there are a few differences that are of interest. Our ZINDO results place the three principally occupied d-based orbitals (with coefficients of 0.84−0.94), $2b_{2g}(d_{xy})$, $2e_g(d_{xz,yz})$, and $9a_{1g}(d_{z^2})$, as the highest three occupied MOs while our ab initio results place them a bit lower, mixed in with π- and p-based orbitals. The ZINDO energies of the virtual orbitals are approximately in the same region as our ab initio results with the notable exceptions of $10a_{1g}$, $9e_u$, and $11a_{1g}$. The $4a_{2u}(p_z, \pi^*)$ and the $6b_{1g}(d_{x^2-y^2}, \sigma^*)$ orbitals switched relative places going from the ab initio to the ZINDO results.

It is interesting to examine the early molecular orbital theory treatment of this and similar complexes by Gray and Ballhausen[2] nearly 40 years ago in light of the results depicted in Figure 4. Their relative energy levels show a remarkable similarity to our ZINDO results with the exception of the low-lying filled orbitals and two of the π-containing mid-level virtual orbitals ($3b_{2g}$ and $2a_{2g}$). The semi-empirical calculation by Zeigler[30] was the first to report using INDO, and the results (which are for filled orbitals only) are remarkably different from the ab initio and ZINDO results.

Allowed Electronic Transitions. The CI that is used for electronic transition calculations in ZINDO considers the effects of reconfigured electrons from several other orbital transitions on the energy of a particular orbital transition. In addition, and not as widely realized, the method combines orbital transitions into state transitions much as an LCAO treatment combines atomic orbitals into molecular orbitals. A critical part of an electronic transition calculation in ZINDO is the choice of the set of orbitals to be considered for CI. The goal is to match the experimental results; conventionally, the CI level is increased until transition energies become stable.[33] The present case, however, illustrates dramatically the effect of variations in the degree of CI and that the CI level should not simply be increased until the transition energies stabilize. Figure 5 shows the solution-equivalent experimental spectrum with composite spectra from 5 levels of CI. Note that CI levels 6 and 9 have $A_{1g} \rightarrow E_u$ state transitions (B) at energies higher than experiment, at 39.3×10^3 and 38.8×10^3 cm^{-1}, respectively. CI = 10 provides an excellent match to the experimental peak at 37.5×10^3 cm^{-1}, and the equivalent transitions from CI = 11 and 14 are significantly lower, at about 32.2×10^3 cm^{-1}. The $A_{1g} \rightarrow A_{2u}$ transition (A) is modeled very accurately by the CI = 6, 9, and 10 calculations, but when the CI level is raised to 11 and 14, the peak red-shifts dramatically.

The reasons for the shifts in energy are apparent from Figure 6 which depicts schematic ground-state orbital energy levels with orbital transition components representing in total at least 97% of the total oscillator strength (from the sum of the squares of the coefficients) of each of the two state transitions of interest. To the left are brackets indicating the orbitals included in the 5 different levels of CI studied, from 6 to 14, and the coefficients of each orbital transition component of the state transitions are listed horizontally for each CI level. The two left-most vertical arrows represent the component orbital transitions for $A_{1g} \rightarrow A_{2u}$, and the remaining arrows are the components for the $A_{1g} \rightarrow E_u$ transition. Where no number is superimposed on a transition, there is no component of that orbital transition from the corresponding CI calculation. Considering first the $A_{1g} \rightarrow A_{2u}$ transition with CI = 10, including orbitals 14−34, there is only 1 orbital transition, $9a_{1g} \rightarrow 4a_{2u}$ (thick red, cross-hatched arrow in Figure 6), that results in an A_{2u} excited state and thus yields the state transition, $A_{1g} \rightarrow A_{2u}$. This calculated transition is compared with the corresponding experimental absorption in Figure 7 where it may be seen that the agreement is excellent. If, however, the CI level is extended beyond 10, orbital 35 becomes included in the calculations and an additional orbital transition, $9a_{1g} \rightarrow 5a_{2u}$ (thin red, crosshatched arrow in Figure 6), becomes combined with the $9a_{1g} \rightarrow 4a_{2u}$ transition. It seems nonintuitive that adding a higher-energy orbital transition should result in a lower state transition unless one draws a parallel to linear

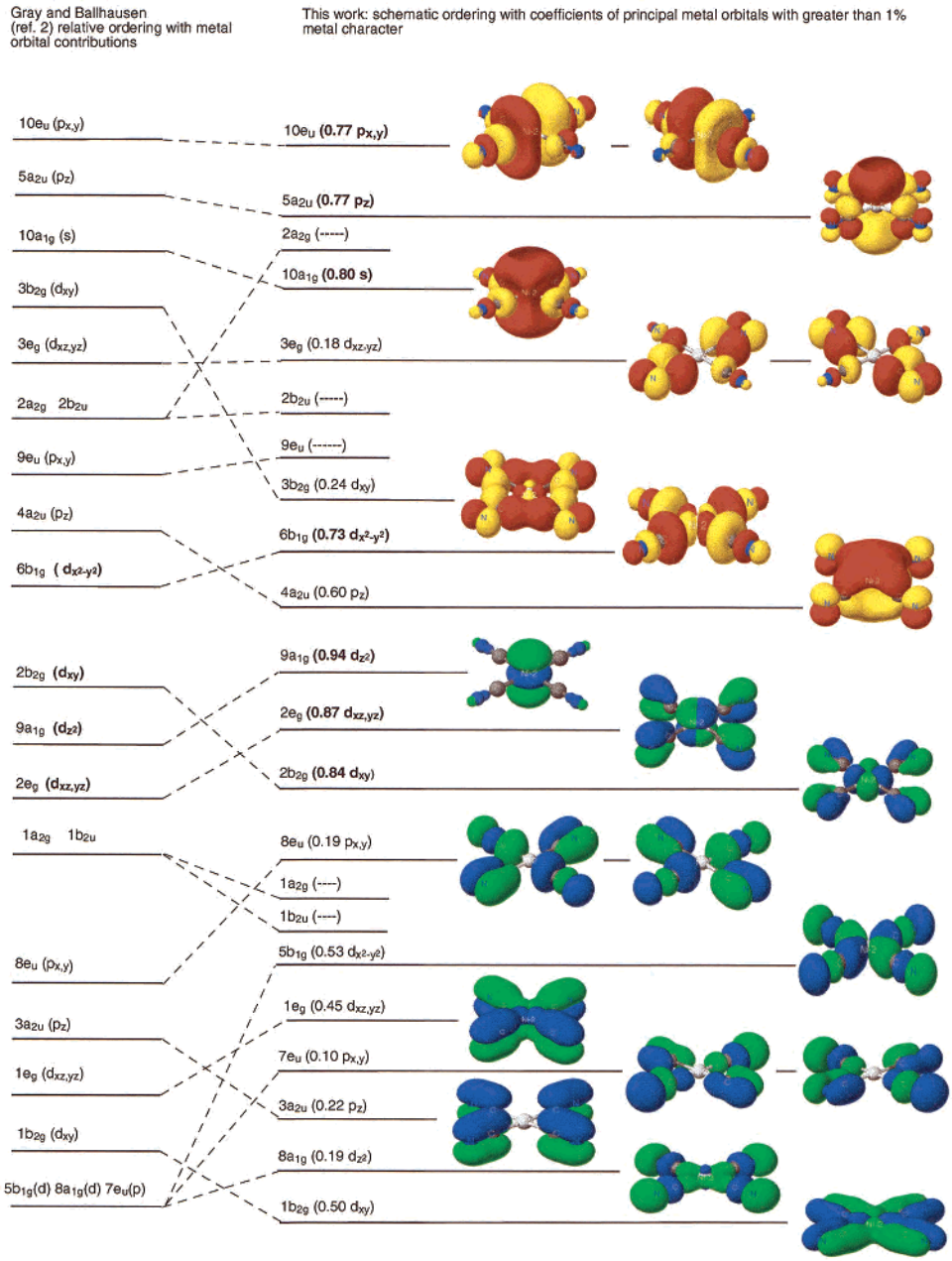

Figure 4. Relative MO ordering of $M(CN)_4^{2-}$ from Gray and Ballhausen[2] compared with the relative ordering from this ZINDO calculation. Included with the ZINDO results are the coefficients of the principal metal orbital; the bold values are the primary contributions from each of the d, s, and p metal orbitals. Also shown are the molecular orbitals that include some metal character.

combinations of atomic orbitals. The actual consequence of the added orbital is that two combinations are formed. Using CI level 11, one combination is $0.94(9a_{1g} \rightarrow 4a_{2u}) + 0.35(9a_{1g} \rightarrow 5a_{2u})$ which appears in Figure 5 at 30.31×10^3 cm^{-1}, with an oscillator strength of 0.081. The other combination is $0.34(9a_{1g} \rightarrow 4a_{2u}) + 0.92(9a_{1g} \rightarrow 5a_{2u})$ which has an energy of 65.46×10^3 cm^{-1}, and an oscillator strength of 0.060. Presumably, the higher energy, 65.46×10^3 cm^{-1}, member of the resultant state transition pair is above the energy of the $9a_{1g} \rightarrow 5a_{2u}$ orbital transition, but the energy of the latter is not available to us. This result illustrates that (1) the guideline of increasing the CI level until the transition energy stabilizes[33] is not always appropriate and (2) state transitions can be a linear combination of orbital transitions. The conclusion regarding the lowest energy *z*-polarized electronic transition is that it is accurately portrayed by a single orbital transition, $9a_{1g} \rightarrow 4a_{2u}$.

The $A_{1g} \rightarrow E_u$ state transition is somewhat more complex because there is a larger number of orbital pairs that can result in the appropriate symmetries in order to contribute to this transition. Looking initially at the CI = 6, 9, and 10 cases, it is clear from Figure 5 that there are significant energy differences between the results for these three CI levels, but as shown in Figure 6, the coefficients for the predominant orbital transition ($2e_g \rightarrow 4a_{2u}$) vary only slightly. While CI = 6 and 9 have the same 3 transitions listed, there is a total of 12 orbital transitions comprising the state transition in the CI = 6 case and 22 in the CI = 9 case (the orbital transitions not listed have coefficients of less than 0.09 and have been deleted for the sake of clarity). It appears

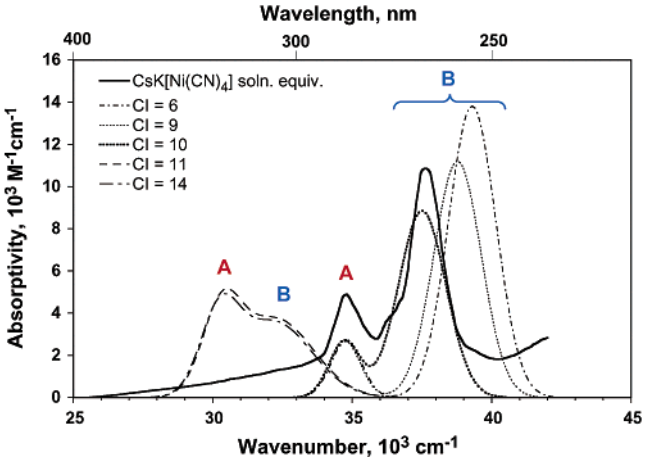

Figure 5. Results of varying the level of configuration interaction (CI), compared with the solution-equivalent spectrum from solid $CsK[Ni(CN)_4]$.[39] Peaks A are the $A_{1g} \rightarrow A_{2u}$ state transitions and peaks B are the $A_{1g} \rightarrow E_u$ transitions.

that the many additional small contributions in the CI = 9 calculation help to change the calculated energy. As can be seen from Figure 5, CI = 10 results in good agreement with experiment. This is more clearly shown in Figure 8, where an *x*,*y*-polarized experimental spectrum is compared with the CI = 10 calculated results for the $A_{1g} \rightarrow E_u$ state transition. It is important to note that for CI = 10, where 10 orbitals below the Fermi level would only include orbitals as low as 15, and exclude one of the $1e_g$ degenerate pair, the ZINDO program automatically includes both members of the pair, so it includes orbital 14 as well. CI = 11 and 14 cause a large red-shift in the transition energy, as with the $A_{1g} \rightarrow A_{2u}$ transition, primarily because of additional orbital transitions to orbital 35, the $5a_{2u}$, with orbital transition coefficients as high as 0.36. Inclusion of this higher energy orbital transition again results in a lower state transition energy as was the case with the *z*-polarized transition. It is clear that inclusion of orbitals outside the range 14−34 does not model reality well. The lowest energy *x*,*y*-polarized electronic transition thus requires several orbital transitions to characterize it. The principal orbital transition, $2e_g \rightarrow 4a_{2u}$, is the one historically assigned to this absorption, including the most recent restatement of this assignment.[41] It is interesting to note, however, that one of the minor but necessary components of the state transition is $2b_{2g} \rightarrow 9e_u$, the orbital transition that we suggested in order to explain the solid-state anomaly in mixed nickel−platinum tetracyano complexes.[40] We will be interested to see the role, if any, that this transition plays in the solid-state modeling we are currently working on.

Real Versus Ideal Structures. We noted earlier that we were required to use an ideal model for the structure of the $Ni(CN)_4^{2-}$ ion. This is due to the fact that, in the real model, the degeneracy of MOs 14 and 15 ($1e_g$) is removed and CI = 10, the best level for the ideal structure, did not automatically include MO 14 in the real molecule calculation. The results are illustrated in Figure 9 where the *z*-polarized transition shows excellent agreement for the ideal and real structures, while the *x*,*y*-polarized transition shows a difference for the two structures. For the ideal structure, the two parts of the degenerate state transition, noted as B(1) and B(2), coincide as expected, while for the real structure, B(1) agrees with the ideal structure but B(2) is at higher energy, resulting in a blue-shifted *x*,*y*-polarized B peak. As suggested by Figure 6 and listed in detail in Table S-6 in the SI, B(1) (listed in Table S-6 as state transition 1 → 7) for the ideal for CI = 10 is $-0.97(2e_g(23) \rightarrow 4a_{2u}(25)) - 0.07(1e_g(20) \rightarrow 3b_{2g}(27)) + 0.06(2b_{2g}(21) \rightarrow 9e_u(29)) + 0.18(1e_g(15) \rightarrow$

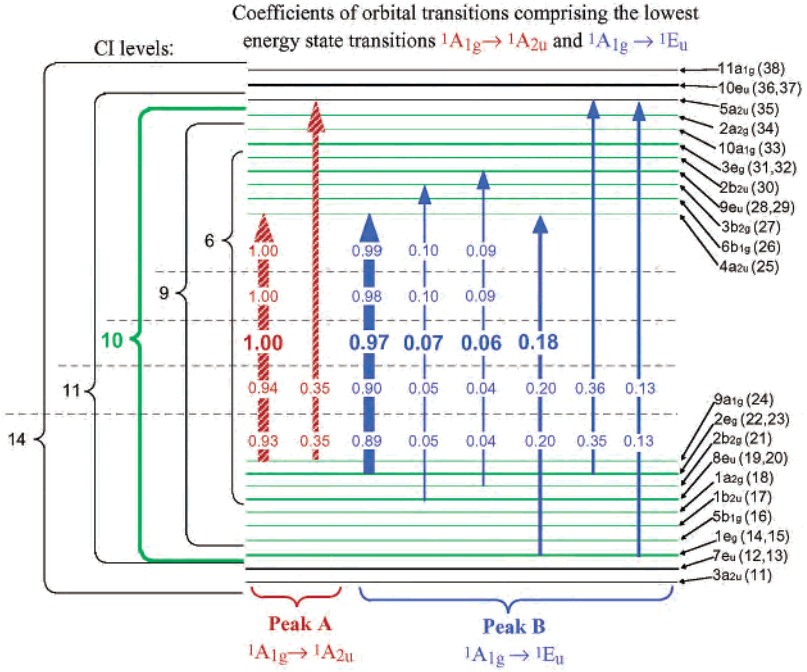

Figure 6. Summary of ZINDO electronic transition calculation results for CI levels 6, 9, 10, 11, and 14. The MO energy levels are schematic only; the two left-most transitions represent the most prominent orbital transitions involved in the $A_{1g} \rightarrow A_{2u}$ state transition, and the other six transitions are the primary orbital transitions comprising the $A_{1g} \rightarrow E_u$ state transition. The values on the transition arrows opposite a 6, 9, etc. are the coefficients for each orbital transition under the CI = 6, 9, etc. level calculation. CI level 10 gave the best fit to experiment.

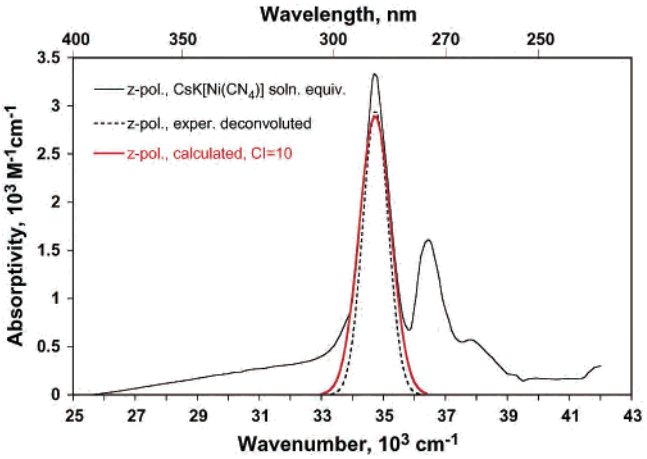

Figure 7. Comparison of the calculated $A_{1g} \rightarrow A_{2u}$ transition with the *z*-polarized spectrum from $CsK[Ni(CN)_4]$ and the corresponding Gaussian curve.

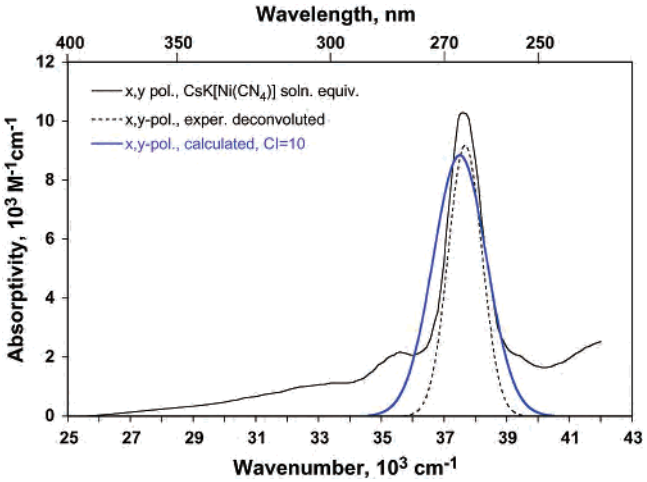

Figure 8. Comparison of the calculated $A_{1g} \rightarrow E_u$ transition with the *x,y*-polarized spectrum from $CsK[Ni(CN)_4]$ and the corresponding Gaussian curve.

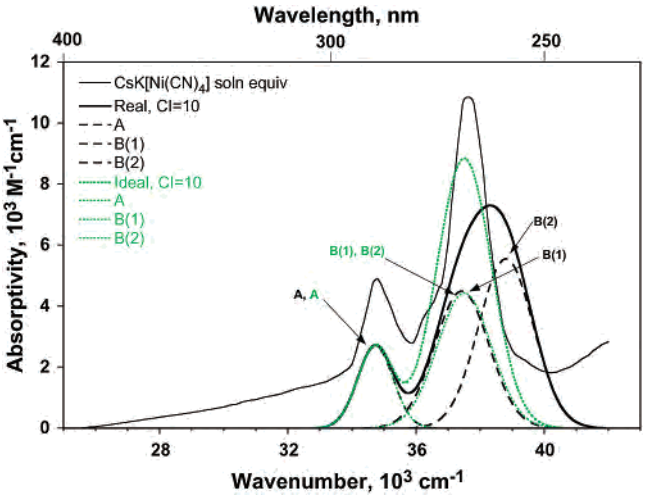

Figure 9. Comparison of ZINDO calculations using an ideal model versus a real model (see text). Both are superimposed on the usual experimental curve.

$4a_{2u}(25)$) and B(2) for the ideal is $0.97(2e_g(22) \rightarrow 4a_{2u}(25)) - 0.07(1e_g(19) \rightarrow 3b_{2g}(27)) + 0.06(2b_{2g}(21) \rightarrow 9e_u(28)) + 0.18(1e_g(14) \rightarrow 4a_{2u}(25))$. B(1) for the real structure is close to that for the ideal. Comparing B(1) and B(2) for the real structure, the most significant difference is that B(2) for the real structure is essentially missing the component $0.18(1e_g(14) \rightarrow 4a_{2u}(25))$. Thus, the real B(2) differs from the ideal B(2) in that orbital 14 is not automatically included because it is not truly degenerate with orbital 15.

The real CI = 10 B(2) peak is, in fact, at the same position as both the ideal and real B(1) and B(2) CI = 9 result (the ideal molecule result is shown in Figure 5) where neither MO 14 nor 15 was included in the configuration interaction. If one were to increase the CI level to 11 in an attempt to include MO 14 in a real molecule calculation, MO 35 would also be included which as Figure 5 also illustrates would result in an incorrect red-shift of both B(1) and B(2), listed simply as B. Ideally, in this system, one would want to have a routine in which an unsymmetrical calculation could be made, where the levels included above and below the Fermi level could be different.

In summary, to answer the question of how the calculation results would have appeared for the real versus ideal models, we can use the results shown in Figures 5 and 9. The *z*-polarized transition at about 34.7×10^3 cm^{-1} is superimposable for the two models. The *x,y*-polarized transition is not as easily compared because of the symmetry considerations discussed in the previous two paragraphs, but the real CI = 10 B(2) peak is in the same position as the ideal CI = 9 B(1) and B(2) = B, around 39.7×10^3 cm^{-1} (see Figure 5). From both the *z*-polarized and *x,y*-polarized results, we can conclude that the ideal model is a very reasonable approximation to the real complex ion.

Conclusions

We have shown that ZINDO calculations provide an excellent fit to experiment for the principal peaks in the $Ni(CN)_4^{2-}$ ion absorption spectrum. The overall conclusion regarding the nature of the lowest two symmetry-allowed transitions is that the earlier assignments are basically correct regarding the principal orbital transitions, but that the $A_{1g} \rightarrow E_u$ state transition at 37.6×10^3 cm^{-1}, while predominately $2e_g \rightarrow 4a_{2u}$, requires minor contributions from $1e_g \rightarrow 4a_{2u}$, $8e_u \rightarrow 3b_{2g}$, and $2b_{2g} \rightarrow 9e_u$ orbital transitions to accurately describe it. Higher-order effects such as spin−orbit coupling are evidently not needed to describe the orbital transitions, judging by the outstanding agreement of our calculated spectra with experiment (Figures 7 and 8).

Acknowledgment. The authors thank Professor Richard Moog at Franklin and Marshall College and Drs. Peter Herman and George Purvis at CAChe Software for helpful discussions. We are grateful to the National Science Foundation for an RUI Grant (CHE9521548) for this work and to Dr. William Hackman for summer research grants through Franklin and Marshall College for one of us (Y.A.M.).

Supporting Information Available: Color depictions of all 41 ZINDO MOs, listing of molecular orbital energies from Gaussian 94, molecular energies and components of state transitions from ZINDO, and parameters used in ZINDO. This material is available free of charge via the Internet at http://pubs.acs.org.

IC025798X